3310 *Inorg. Chem.* **2010**, *49*, 3310–3319
DOI: 10.1021/ic902243q

Inorganic Chemistry
Article

Controlling the Reactivity of Ruthenium(II) Arene Complexes by Tether Ring-Opening

Ana M. Pizarro,[†] Michael Melchart,[‡] Abraha Habtemariam,[†] Luca Salassa,[†] Francesca P. A. Fabbiani,[‡] Simon Parsons,[‡] and Peter J. Sadler*[,†]

[†]*Department of Chemistry, University of Warwick, Gibbet Hill Road, Coventry CV4 7AL, U.K., and* [‡]*School of Chemistry, University of Edinburgh, West Mains Road, Edinburgh EH9 3JJ, U.K.*

Received November 18, 2009

The closed- and open-tethered Ru^{II} η^6-arene complexes $[Ru^{II}(\eta^6{:}\eta^1\text{-}C_6H_5(C_6H_4)NH_2)(en)]Cl_2$ (**2**) and $[Ru^{II}(\eta^6\text{-}C_6H_5(C_6H_4)NH_2)Cl(en)]Cl$ (**3**), where en is ethylenediamine, have been synthesized and their X-ray structures determined. Interconversion between **2** and **3**, that is, tethered-arene ring-closure and ring-opening, in different solvents has been investigated. Complex **2** opens in dimethylsulfoxide (DMSO) by solvent-induced dissociation of the NH_2 group of the pendant arm. In methanol, however, equilibrium between **2** and **3** is reached after 12 h when both species coexist in solution in a ratio of 2:1 (open/closed). In water (pH 7), complete ring closure of **3** to **2** at 298 K occurs in less than 2 h. The tether ring of complex **2** opens at basic pH and closes at neutral pH. Complex **2** opens over time (18 h) in concentrated HCl. The opening-closing process is fully reversible in the pH range 2−12. Density Functional Theory calculations have been used to obtain insights into the electronic structure of complexes **2** and **3**, their UV−vis properties, and their stability compared to their aqua derivatives. Control of tether-ring-opening can contribute toward a strategy for activation and for achieving cytotoxic selectivity of ruthenium arene anticancer drugs.

Introduction

Organometallic Ru η^6-arene complexes have well-known applications in catalysis[1] and are of increasing medicinal interest.[2−4] Complexes of general formula $[Ru^{II}(\eta^6\text{-arene})(XY)Z]$, where XY is a chelating ligand and Z a labile ligand, have shown encouraging potential as anticancer agents.[5] The activation of these complexes through hydrolysis of the Ru−Z bond is highly dependent on the degree of lability of the leaving group, leading to activity in both catalysis and nucleotide binding.[6] Therefore, controlling the activation of these bonds can provide a strategy for achieving cytotoxic selectivity and contribute toward the rational design process.

Organometallic transition metal complexes with a potential coordinating atom such as nitrogen, oxygen, and phosphorus tethered to a η^6-arene ligand have been reported previously. For example, Scolaro et al. have investigated the effect of different functionalized arenes in potentially cytotoxic Ru-arene complexes on their ability to form hydrogen bonds, and the relationship to cell uptake, DNA binding, and cytotoxicity.[7] Also, Miyaki et al. have investigated the formation and the stability of several organometallic arene ruthenium catalysts containing a pendant aliphatic arm with a chelating heteroatom.[8] Furthermore, Melchart et al. synthesized a series of tethered neutral Ru^{II} complexes of general formula $[Ru^{II}(\eta^6{:}\eta^1\text{-arene:N})Cl_2]$, as well as the more stable derivatives $[Ru^{II}(\eta^6{:}\eta^1\text{-arene:N})(oxalate)]$, and investigated their stability with regard to arene loss in solution and suitability as cytotoxic bifunctional ruthenium agents.[9,10] In the pursuit of controlled metal-complex activation, Habtemariam et al. reported chelate ring-opening/closing

*To whom correspondence should be addressed. E-mail: p.j.sadler@warwick.ac.uk.

(1) Noyori, R.; Ohkuma, T.; Sandoval, C. A.; Muniz, K. *Asymmetric Synth.* **2007**, 321–325.
(2) Melchart, M.; Sadler, P. J. In *Bioorganometallics*; Jaouen, G., Ed.; Wiley-VCH: Weinheim, Germany, 2006; pp 39−64.
(3) Peacock, A. F. A.; Sadler, P. J. *Chem.—Asian J.* **2008**, *3*, 1890–1899.
(4) Renfrew, A. *Chimia* **2009**, *63*, 217–219.
(5) Habtemariam, A.; Melchart, M.; Fernandez, R.; Parsons, S.; Oswald, I. D. H.; Parkin, A.; Fabbiani, F. P. A.; Davidson, J. E.; Dawson, A.; Aird, R. E.; Jodrell, D. I.; Sadler, P. J. *J. Med. Chem.* **2006**, *49*, 6858–6868.
(6) Wang, F.; Habtemariam, A.; van der Geer, E. P. L.; Fernandez, R.; Melchart, M.; Deeth, R. J.; Aird, R.; Guichard, S.; Fabbiani, F. P. A.; Lozano-Casal, P.; Oswald, I. D. H.; Jodrell, D. I.; Parsons, S.; Sadler, P. J. *Proc. Natl. Acad. Sci. U.S.A.* **2005**, *102*, 18269–18274.
(7) Scolaro, C.; Geldbach, T. J.; Rochat, S.; Dorcier, A.; Gossens, C.; Bergamo, A.; Cocchietto, M.; Tavernelli, I.; Sava, G.; Rothlisberger, U.; Dyson, P. J. *Organometallics* **2006**, *25*, 756–765.
(8) Miyaki, Y.; Onishi, T.; Kurosawa, H. *Inorg. Chim. Acta* **2000**, *300−302*, 369–377.
(9) Melchart, M.; Habtemariam, A.; Novakova, O.; Moggach, S. A.; Fabbiani, F. P. A.; Parsons, S.; Brabec, V.; Sadler, P. J. *Inorg. Chem.* **2007**, *46*, 8950–8962.
(10) Melchart, M. Ph.D. Thesis, University of Edinburgh, **2006**.

 Published on Web 03/05/2010

for square-planar bis(aminophosphine)platinum(II) and palladium(II) complexes.[11] They were able to control the dynamics of the chelate formation, which was dependent not only on the substituents and length of the tether but also on the pH and chloride concentration of the aqueous solution.

Transition metal complexes with hemilabile chelating ligands containing mixed funtionalities have been shown to have potential applications as precursors in catalytic processes, small-molecule activation, and molecule-based sensors in recent years.[12,13] The hemilability of a chelate can be described as a (reversible) dynamic process that involves dissociation and recoordination to the metal center of a weakly bound donor.

In this work we have studied a Ru-arene complex with a hemilabile amino-derivatized arene ligand, where the η^6-bound arene is inert to substitution but the amino group offers two reversible functionalities: (i) binding to the Ru^{II} center to form a tether-ring-closed (inactivated) complex, or (ii) dissociation of the amine from the Ru^{II} center (as a dangling arm) to afford an open-tether complex with a pendant free amino group. In the open form the vacant site on the ruthenium is occupied by either chloride or a solvent molecule (activated complex). In aqueous solution, the tether-ring dynamics are pH dependent, giving the potential to finely tune the activation process to biological conditions, for example, the acidic environment of the tumor.[14]

We have investigated the interconversion of the inactive closed-ring complex [Ru(η^6:η^1-$C_6H_5(C_6H_4)NH_2$)(en)]Cl_2, **2**, and its activated open-tether ruthenium complex, [Ru(η^6-$C_6H_5(C_6H_4)NH_2$)Cl(en)]Cl, **3**, (as a function of the solvent and pH), which can offer a vacant site on the metal ion for substrate binding, with the aim of controlling the binding availability of such Ru^{II}-arene derivatives.

Experimental Section

Materials. The diolefin ethyl-1,4-cyclohexadiene-3-carboxylate and [Ru(η^6-etb)Cl_2]$_2$ (etb = ethyl benzoate) were prepared as described elsewhere.[9,15] 2-Aminobiphenyl, ethylenediamine, tetrahydrofuran (THF), *tert*-butylmethyl ether, $(CD_3)_2SO$ (99%), CD_3OD (99.8%) and D_2O (99.9%) were purchased from Sigma-Aldrich. Ethylenediamine was distilled over sodium prior to use. $RuCl_3 \cdot nH_2O$ was purchased from Precious Metals Online PMO Pty Ltd. and from Alfa Aesar. Hydrochloric acid, 1,4-dioxane, 1,2-dichloroethane, acetone, diethyl ether, methanol, and ethanol were supplied by Fisher Scientific. Ethanol was dried over Mg/I_2.

Preparations. [Ru(η^6:η^1-$C_6H_5(C_6H_4)NH_2$)Cl_2] (1). [Ru(η^6-etb)Cl_2]$_2$ (510 mg, 0.79 mmol) and 2-aminobiphenyl (270 mg, 1.60 mmol) were suspended in 1,2-dichloroethane (50 mL). The mixture was stirred for 45 min at ambient temperature giving a red solution. THF (2 mL) was added, and the mixture degassed with argon for 30 min. The vessel was closed, and the reaction mixture heated under pressure at 393 K for 18 h. The dark red-brown, air-stable microcrystalline material was collected by filtration, washed with acetone and diethyl ether, and dried in air (488 mg, 90% yield). Anal. Calcd for $C_{12}H_{11}Cl_2NRu$: C, 42.24; H, 3.25; N, 4.11. Found: C, 41.80; H, 3.11; N, 3.96. ESI-HR-MS (*m*/*z*): calcd for $\{C_{12}H_{11}Cl_2NRu + Na\}^+$, 363.9201; found, 363.9202 (100%).

[Ru(η^6-$C_6H_5(C_6H_4)NH_3$)Cl_3] (1·HCl). Complex **1**, [Ru(η^6:η^1-$C_6H_5(C_6H_4)NH_2$)Cl_2], (118 mg, 0.35 mmol) was suspended in concentrated HCl (ca. 12 M, 15 mL) and left stirring at ambient temperature in the dark for 18 h. Red crystals suitable for X-ray diffraction were collected by filtration and washed with 1 M HCl, ethanol and ether. Yield: 98 mg (75%). ^{1}H NMR (DMSO-d_6): δ 7.38 (d, 1H, J = 7.5 Hz), δ 7.16 (t, 1H, J = 7.5 Hz), δ 6.79 (d, 1H, J = 7.5 Hz), δ 6.67 (t, 1H, J = 7.5 Hz), δ 6.22 (d, 2H, J = 6 Hz), δ 6.13 (t, 1H, J = 6 Hz), δ 5.95 (t, 2H, J = 6 Hz), δ 5.42 (bs, 2H). Anal. Calcd for $C_{12}H_{12}Cl_3NRu$: C, 38.16; H, 3.20; N, 3.71. Found: C, 38.45; H, 3.26; N, 3.76.

[Ru(η^6:η^1-$C_6H_5(C_6H_4)NH_2$)(en)]Cl_2 (2). Complex **1**, [Ru(η^6:η^1-$C_6H_5(C_6H_4)NH_2$)Cl_2], (119 mg, 0.35 mmol) was suspended in 95% aqueous methanol (2 mL). Ethylenediamine (28 μL, 0.42 mmol) was added, and the mixture was stirred for 2 h at ambient temperature. The solvent was removed in vacuo, and complex **2** was isolated as a yellow powder. Yield: 49%. X-ray diffraction quality crystals were obtained after reducing the volume of the reaction mixture to one-quarter on a rotary evaporator and storing at 277 K for 18 h. Yellow crystals were obtained from the cold methanol solution affording the structure of complex **2**. ^{1}H NMR (methanol-d_4): δ 7.66 (d, 1H, J = 7.5 Hz), δ 7.56 (t, 1H, J = 7.5 Hz), δ 7.51 (t, 1H, J = 7.5 Hz), δ 7.45 (d, 1H, J = 7.5 Hz), δ 6.23 (t, 2H, J = 6 Hz), δ 5.66 (d, 2H, J = 6 Hz), δ 5.50 (t, 1H, J = 6 Hz), δ 2.67 (m, 2H), δ 2.52 (m, 2H). ^{13}C NMR (D_2O; 1,4-dioxan): δ 148.9, 135.7, 130.2, 128.1, 127.1, 126.0, 109.8, 90.8, 77.8, 72.6, 45.0, 44.9. Anal. Calcd for $C_{12}H_{19}Cl_2N_3Ru$: C, 41.90; H, 4.77; N, 10.47. Found: C, 40.97; H, 4.80; N, 10.79. ESI-MS (*m*/*z*): $\{C_{14}H_{19}N_3Ru - H\}^+$, 330.0 (100%).

[Ru(η^6-$C_6H_5(C_6H_4)NH_2$)Cl(en)]Cl (3). Complex **1**, [Ru(η^6:η^1-$C_6H_5(C_6H_4)NH_2$)Cl_2], (119 mg, 0.35 mmol) was suspended in 95% aqueous methanol (2 mL). Ethylenediamine (28 μL, 0.42 mmol) was added, and the mixture was stirred for 2 h at ambient temperature. The solvent was reduced to approximately 0.5 mL on a rotary evaporator, and the concentrated solution was stored at 277 K for 18 h. Yellow crystals of complex **2** were filtered off from the cold methanol solution. A second batch of orange crystals grew after a few days by slow gas diffusion of *tert*-butylmethyl ether into the methanolic filtrate at 277 K. The crystals obtained were suitable for X-ray analysis. ^{1}H NMR (methanol-d_4): δ 7.42 (d, 1H, J = 7.5 Hz), δ 7.21 (t, 1H, J = 7.5 Hz), δ 6.86 (d, 1H, J = 7.5 Hz), δ 6.81 (t, 1H, J = 7.5 Hz), δ 6.03 (d, 2H, J = 6 Hz), δ 5.99 (t, 1H, J = 6 Hz), δ 5.70 (t, 2H, J = 6 Hz), δ 2.53 (m, 2H), δ 2.39 (m, 2H).

[Ru(η^6-$C_6H_5(C_6H_4)NH_2$)(DMSO-d_6)(en)]Cl_2 (4). Complex **2**, [Ru(η^6:η^1-$C_6H_5(C_6H_4)NH_2$)(en)]Cl_2, (2.3 mg, 5.7 μmol) was dissolved in a minimum amount of DMSO-d_6 (ca. 100 μL) and left standing overnight at ambient temperature. Complex **4** precipitated out of solution when 1.5 mL of diethyl ether was added. The solvent was removed from the brown solid by centrifugation, washed with ether, and dried in air. ^{1}H NMR (DMSO-d_6): δ 7.38 (d, 1H, J = 7.5 Hz), δ 7.13 (t, 1H, J = 7.5 Hz), δ 6.79 (t, 1H, J = 7.5 Hz), δ 6.67 (d, 1H, J = 7.5 Hz), δ 6.60 (bs, 2H), δ 6.00 (t, 1H, J = 6 Hz), δ 5.97 (d, 2H, J = 6 Hz), δ 5.67 (t, 2H, J = 6 Hz), δ 5.28 (s, 2H), δ 4.11 (bs, 2H), δ 2.30 (m, 2H), δ 2.23 (m, 2H). ^{13}C NMR (DMSO-d_6): δ 146.8, 131.8, 130.2, 130.2, 118.8, 117.5, 116.5, 97.8, 86.2, 84.1, 79.9, 44.7. IR (ν_{S-O}): 1101 cm^{-1}.

Methods and Instrumentation

(a). X-ray Crystallography. Diffraction data for compounds **1·HCl**, **2**, and **3** were collected at 150 K using a Bruker Smart Apex CCD diffractometer. Absorption corrections for all data sets were performed with the multiscan procedure SADABS.[16]

(11) Habtemariam, A.; Watchman, B.; Potter, B. S.; Palmer, R.; Parsons, S.; Parkin, A.; Sadler, P. J. *J. Chem. Soc., Dalton Trans.* **2001**, 1306–1318.
(12) Slone, C. S.; Weinberger, D. A.; Mirkin, C. A. *Prog. Inorg. Chem.* **1999**, *48*, 233–350.
(13) Bader, A.; Lindner, E. *Coord. Chem. Rev.* **1991**, *108*, 27–110.
(14) Griffiths, J. R. *Br. J. Cancer* **1991**, *64*, 425–427.
(15) Therrien, B.; Ward, T. R.; Pilkington, M.; Hoffmann, C.; Gilardoni, F.; Weber, J. *Organometallics* **1998**, *17*, 330–337.
(16) Sheldrick, G. M. *SADABS 2001−2004*; University of Gottingen: Gottingen, Germany, 2006.

The structure of **1·HCl** was solved by direct methods (SIR92),[17] and that of **2** and **3** by Patterson methods (DIRDIF).[18] Refinement was against F^2 using all data (CRYSTALS[19] for **1·HCl** and **2** and SHELXL[20] for **3**). Hydrogen atoms attached to nitrogen were found in difference maps, and the pattern of H-bonding in the two structures is consistent with the positions suggested. In **3**, H-atoms on N11 were refined subject to the restraint that the two NH distances are equal. All non-H atoms were refined with anisotropic displacement parameters. The programs ChemCraft,[21] Mercury 1.4.1,[22] and ORTEP 32[23] were used for analysis of data and production of graphics.

The crystal structures of **1·HCl**, **2**, and **3** have been deposited in the Cambridge Crystallographic Data Center under the accession numbers CCDC 752219, 752220, and 752221, respectively.

(b). NMR Spectroscopy. ^{1}H NMR spectra were acquired for samples in 5 mm NMR tubes at 298 K on either a Bruker DMX 500 or a Bruker AVA 600 NMR spectrometer, using TBI [^{1}H, ^{13}C, X] or TXI [^{1}H, ^{13}C, X] probeheads equipped with *z*-field gradients. All of the data processing was carried out using TOPSPIN version 2.0 (Bruker U.K. Ltd.). ^{1}H NMR chemical shifts were internally referenced to TSP via 1,4-dioxane (δ 3.76) for aqueous solutions, CHD_2OD (δ 3.31) for methanol-d_4 or $(CHD_2)(CD_3)SO$ for DMSO-d_6 (δ 2.50). 1D and 2D spectra were recorded using standard pulse sequences, which were modified by Dr. Dusan Uhrin and Mr. Juraj Bella, at the University of Edinburgh. Water signals were suppressed using presaturation or Shaka methods.[24] All the experiments followed by NMR were carried out in deuterated solvent at 298 K, with exception of the experiment in aqueous solution where the solvent was 90% H_2O/10% D_2O. Typically, 1 mg of complex was dissolved in 1 mL of the solvent (ca. 2.5 mM), and 600 μL of this solution was added to a 5 mm NMR tube.

(c). Elemental Analysis. CHN elemental analyses were performed on a CE-440 Elemental Analyzer by Exeter Analytical (U.K.) Ltd.

(d). MS. Electrospray ionization mass spectra (ESI-MS) were obtained on a Micromass Platform II mass spectrometer, and aqueous solutions were infused directly. The capillary voltage was 3.5 V, and the cone voltage was varied between 20 and 45 V depending on sensitivity. The source temperature was 353 K. Mass spectra were recorded with a scan range of m/z 250−1200 for positive ions. High resolution MS data were obtained using a Bruker MicroTOF, Bruker MaXis mass spectrometer.

(e). IR. FT-IR spectra were acquired at ambient temperature as dimethylsulfoxide (DMSO) solutions (4000−600 cm^{-1}) on a Perkin-Elmer Paragon 1000 spectrometer.

(f). Analysis of Tethered-Arene Ring-Opening/Closure in Solution. In the time-course ^{1}H NMR experiments, the time of dissolution of the reactants was taken as $t = 0$. ^{1}H NMR spectra were recorded at convenient intervals until no further changes were observed.

The data of the time-course dynamics of the tethered chelate in different solvents, based on peak integrals, were fitted to the appropriate kinetic equation. OriginPro 8 SR2 (OriginLab Corp., MA, U.S.A.) was used to fit the exponential decay and to obtain the rate constant.

(g). pH Titrations. The pH titrations were followed by NMR and UV−visible spectroscopy. Experiments were carried out at 298 K. The pH values were adjusted with dilute $HClO_4$ or HNO_3 for the acidic titration, and with KOH or NaOH for the basic titration.

NMR Spectroscopy. The spectra were recorded at pH values measured at about 298 K directly in the NMR tube, before and after recording the ^{1}H NMR spectra, using a Corning 145 pH meter equipped with an Aldrich micro combination electrode, calibrated with Aldrich buffer solutions at pH 4, 7, and 10.

UV−vis Spectroscopy. An aqueous solution of complex **2** (830 μM) was prepared. pH values of the solution in H_2O were measured at about 298 K, before and after recording the spectra. UV−vis spectra were recorded on a Varian Cary 300 UV−visible spectrophotometer using 1 cm path-length quartz cuvettes (volume 0.5 mL). Data were processed with OriginPro 8 SR2 (OriginLab Corp., MA, U.S.A.).

(h). Computational Details. All calculations were performed with the Gaussian 03 (G03) program[25] employing the Density Functional Theory (DFT) method. For complexes **2** and **3** the correlation functionals PBE1PBE[26] and B3LYP[27,28] were used with the LanL2DZ basis set[29] and effective core potential for the Ru atom and the 6-31G** basis set[30] for all other atoms. Geometry optimizations of **2** and **3** in the ground state were performed in the gas phase. Furthermore, geometry optimization at the PBE1PBE/LanL2DZ/6-31G** level of **2** plus a Cl^- counterion [**2**+**Cl**] and **2** plus a H_2O molecule [**2**+**H_2O**] were obtained to compare the stability of complexes **2**, **3**, and [**5**+**H**] (coordinated H_2O instead of OH^-). The nature of all stationary points was confirmed by normal-mode analysis. The conductor-like polarizable continuum model method (CPCM)[31] with water as solvent was used to calculate the electronic structure and the excited states of **2** and **3**, [**2**+**Cl**] and **5** in aqueous solution. Thirty-two singlet excited states and the corresponding oscillator strengths were determined with a time dependent DFT (TD-DFT)[32,33] calculation. Only selected electronic transitions are reported. The electronic distribution and the localization of the singlet excited states were visualized using electron density difference maps (EDDMs).[34−36] GaussSum 1.05[37] was used for EDDMs calculations and for the electronic spectrum simulation. Results of all calculations are summarized in detail in the Supporting Information Section.

(17) Altomare, A.; Cascarano, G.; Giacovazzo, C.; Guagliardi, A.; Burla, M. C.; Polidori, G.; Camalli, M. *J. Appl. Crystallogr.* **1994**, *27*, 435.
(18) Beurskens, P. T.; Beurskens, G.; Bosman, W. P.; De Gelder, R.; Garcia-Granda, S.; Gould, R. O.; Israel, R.; Smits, J. M. M. *The DIRDIF96 Program System*; University of Nijmegen: Nijmegen, The Netherlands, 1996.
(19) Betteridge, P. W.; Carruthers, J. R.; Cooper, R. I.; Prout, K.; Watkin, D. J. *J. Appl. Crystallogr.* **2003**, *36*, 1487.
(20) Sheldrick, G. M. *SHELXL-97 Program for the refinement of crystal structures*; University of Gottingen: Gottingen, Germany, 1997.
(21) Zhurko, G. A. http://www.chemcraftprog.com.
(22) Macrae, C. F.; Edgington, P. R.; McCabe, P.; Pidcock, E.; Shields, G. P.; Taylor, R.; Towler, M.; van de Streek, J. *J. Appl. Crystallogr.* **2006**, *39*, 453–457.
(23) Farrugia, L. J. *J. Appl. Crystallogr.* **1997**, *30*, 565.
(24) Hwang, T.-L.; Shaka, A. J. **1995**, *112*, 275−279.
(25) Frisch, M. J. et al. *GAUSSIAN 03* (Revision D.01); Gaussian, Inc., Wallingford, CT, 2004.
(26) Perdew, J. P.; Burke, K.; Ernzerhof, M. *Phys. Rev. Lett.* **1996**, *77*, 3865–3868.
(27) Becke, A. D. *J. Chem. Phys.* **1993**, *98*, 5648–5652.
(28) Lee, C.; Yang, W.; Parr, R. G. *Phys. Rev. B: Condens. Matter* **1988**, *37*, 785–789.
(29) Hay, P. J.; Wadt, W. R. *J. Chem. Phys.* **1985**, *82*, 270–283.
(30) McLean, A. D.; Chandler, G. S. *J. Chem. Phys.* **1980**, *72*, 5639–5648.
(31) Cossi, M.; Rega, N.; Scalmani, G.; Barone, V. *J. Comput. Chem.* **2003**, *24*, 669–681.
(32) Casida, M. E.; Jamorski, C.; Casida, K. C.; Salahub, D. R. *J. Chem. Phys.* **1998**, *108*, 4439–4449.
(33) Stratmann, R. E.; Scuseria, G. E.; Frisch, M. J. *J. Chem. Phys.* **1998**, *109*, 8218–8224.
(34) Browne, W. R.; O'Boyle, N. M.; McGarvey, J. J.; Vos, J. G. *Chem. Soc. Rev.* **2005**, *34*, 641–663.
(35) Albertino, A.; Garino, C.; Ghiani, S.; Gobetto, R.; Nervi, C.; Salassa, L.; Rosenberg, E.; Sharmin, A.; Viscardi, G.; Buscaino, R.; Croce, G.; Milanesio, M. *J. Organomet. Chem.* **2007**, *692*, 1377–1391.
(36) Garino, C.; Gobetto, R.; Nervi, C.; Salassa, L.; Rosenberg, E.; Ross, J. B. A.; Chu, X.; Hardcastle, K. I.; Sabatini, C. *Inorg. Chem.* **2007**, *46*, 8752–8762.
(37) O'Boyle, N. M.; Vos, J. G. *GaussSum*; Dublin City University: Dublin City, Ireland, 2005. Available at http://gausssum.sourceforge.net.

Chart 1. Ruthenium(II) Arene Complexes Studied in This Work

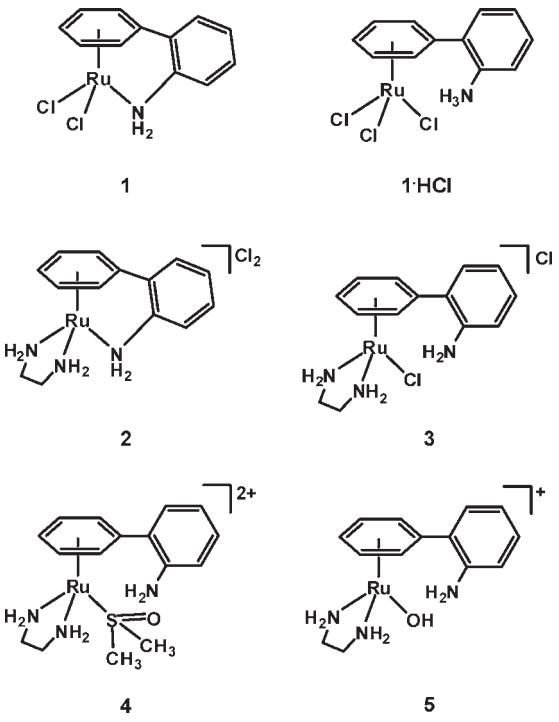

Results

Synthesis and Characterization. The synthesis of the amino-tethered dichlorido Ru^{II} arene complex **1**, [Ru(η^6:η^1-$C_6H_5(C_6H_4)NH_2$)Cl_2], was based on a variation of a published method.[9,15] The thermal displacement of ethyl benzoate in the dimer [Ru(η^6-etb)Cl_2]$_2$ (etb = ethyl benzoate) by 2-aminobiphenyl in 1,2-dichloroethane under pressure resulted in the formation of complex **1**.

Reaction of **1** with 12 M HCl for 18 h at ambient temperature afforded X-ray quality crystals of complex **1·HCl**. Reaction of [Ru(η^6:η^1-$C_6H_5(C_6H_4)NH_2$)Cl_2] (**1**) and [Ru(η^6-$C_6H_5(C_6H_4)NH_3$)Cl_3] (**1·HCl**) with ethylenediamine in aqueous methanol at ambient temperature gave [Ru(η^6:η^1-$C_6H_5(C_6H_4)NH_2$)(en)]Cl_2 (**2**) as a yellow powder after removal of the solvent. In the case of **1·HCl**, a 30% mol excess of the diamine was required to afford complex **2** in low yield. Isolation of the open-tether [Ru(η^6-$C_6H_5(C_6H_4)NH_2$)Cl(en)]Cl (**3**) from methanolic solutions by standard purification techniques was unsuccessful on account of its hygroscopic nature. Only through the growth of crystals could pure complex **3** be isolated, in low yield, and X-ray determination was crucial in the unequivocal assignment of its structure.

CHN elemental analysis, ^{1}H NMR, and IR spectroscopy were used to characterize complexes **1**−**3**, including **1·HCl**, (Chart 1). X-ray crystallography aided the characterization of complexes **1·HCl**, **2**, and **3**.

The ^{1}H NMR signals of the η^6-bound arene for complexes **1·HCl**, **2**, **3**, **4**, and **5** are shifted to high field (by up to ca. 2 ppm) and of the unbound phenyl ring on the tethered arm for complexes **1·HCl**, **3**, **4**, and **5** (open tethers) to low field, by up to about 0.3 ppm and by up to 0.8 ppm for complex **2** (closed tether), compared to the free ligand in the same solvent. Assignment for complexes **2** and **4** in DMSO-d_6 was carried out by analysis of the amine protons peaks of the pendant-arm NH_2, in the two-dimensional (2D) [^{1}H,^{1}H] NOESY NMR spectrum. The closed tether (**2**) showed NOE correlations between the NH_2 of the tether and the NH_2(en) and the CH_2(en) signals. The open tether (**4**) showed no NOE correlations for the NH_2 of the tether. A cross peak between the NH_2 of the tether and the signal of residual water in DMSO-d_6, indicated that these protons exchange chemically with one another.

Complex **4**, [Ru(η^6-$C_6H_5(C_6H_4)NH_2$)(DMSO-d_6)(en)]$^{2+}$, was isolated by precipitation, characterized by NMR (see Supporting Information, Figure S1) and IR spectroscopy but was not further purified. The IR spectrum of complex **4** showed a band at 1101 cm^{-1} assignable to the S−O stretching frequency for S-bonded sulphoxide.[38] This is at higher frequency compared to the free ligand (ν_{S-O} = 1050 cm^{-1}), thus confirming unequivocally that the DMSO is bound through the S.[39,40] S-coordination of DMSO has been reported to predominate in Ru^{II}(η^6-arene) species.[41−44]

Complex **5**, [Ru(η^6-$C_6H_5(C_6H_4)NH_2$)(en)(OH)]$^+$, was formed during a basic titration, by adding strong base (0.1 M NaOH) to an aqueous solution of complex **2** (vide infra). It was characterized by ^{1}H NMR in aqueous solution at pH > 9 (see Supporting Information, Figure S2). The ^{1}H NMR signals of the unbound arene appeared at 7.39−6.98 ppm and those assignable to the bound arene at 5.88−5.70 ppm. The amine proton signals for the en ligand were at 6.02 and 3.47 ppm, for the NH proton pointing up toward the arene ligand and down away the arene ligand, respectively. The CH_2(en) proton signals appeared as a complex signal centered at 2.48 ppm. Characterization of **5** was further confirmed by UV−vis spectra (experimental and theoretical by DFT calculations), where an intense ligand-centered (2-aminophenyl) transition at about 300 nm appearing at pH > 10 confirms the presence of the open tether (vide infra).

X-ray Crystal Structures and DFT-Optimized Geometries. The X-ray crystal structures of [Ru(η^6-$C_6H_5(C_6H_4)NH_3$)Cl_3] (**1·HCl**), [Ru(η^6:η^1-$C_6H_5(C_6H_4)NH_2$)(en)]Cl_2 (**2**), and [Ru(η^6-$C_6H_5(C_6H_4)NH_2$)Cl(en)]Cl (**3**) were determined. Their structures and atom numbering schemes are shown in Figure 1. Crystallographic data and selected bond lengths and angles are shown in Tables 1 and 2, respectively. The complexes adopt the expected pseudo-octahedral "three-legged piano-stool" geometry with the ruthenium η^6-bonded to the arene ligand (Ru to centroid of bound ring, 1.65−1.67 Å), and σ-bonded to three additional ligands which constitute the three legs of the stool. For compound **1·HCl**, the three ligands are three chlorides (2.41−2.44 Å), for compound **2** and **3** two of the three positions are occupied by two nitrogen

(38) Nakamoto, K. *Infrared and Raman Spectra of Inorganic and Coordination Compounds*; John Wiley: New York, 1986.
(39) Bora, T.; Singh, M. M. *Trans. Met. Chem.* **1978**, *3*, 27–31.
(40) Alessio, E.; Balducci, G.; Calligaris, M.; Costa, G.; Attia, W. M.; Mestroni, G. *Inorg. Chem.* **1991**, *30*, 609–618.
(41) Chen, H. Ph.D. Thesis, University of Edinburgh, **2003**.
(42) Beasley, T. J.; Brost, R. D.; Chu, C. K.; Grundy, S. L.; Stobart, S. R. *Organometallics* **1993**, *12*, 4599–4606.
(43) Chandra, M.; Pandey, D. S.; Puerta, M. C.; Valerga, P. *Acta Crystallogr., Sect. E: Struct. Rep. Online* **2002**, *E58*, m28–m29.
(44) Mashima, K.; Kaneko, S.-i.; Tani, K.; Kaneyoshi, H.; Nakamura, A. *J. Organomet. Chem.* **1997**, *545*−*546*, 345–356.

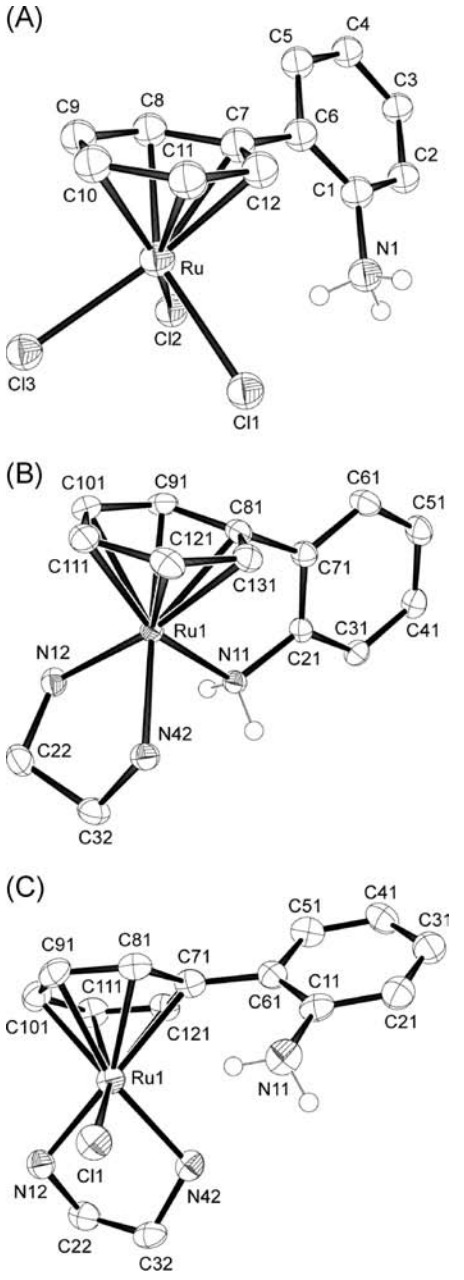

Figure 1. X-ray structures and atom numbering schemes for complexes (A) $[Ru^{II}(\eta^6\text{-}C_6H_5(C_6H_4)NH_3)Cl_3]$, **1·HCl**; (B) $[Ru^{II}(\eta^6{:}\eta^1\text{-}C_6H_5(C_6H_4)NH_2)(en)]Cl_2$, **2**; and (C) $[Ru^{II}(\eta^6\text{-}C_6H_5(C_6H_4)NH_2)Cl(en)]Cl$, **3**; 50% probability ellipsoids. The H atoms (except on the nitrogen pendant from the tether) and counterions are omitted for clarity.

atoms of the ethylenediamine chelate (2.12−2.14 Å). The third position is occupied by a nitrogen, pendant from the tethered arene in **2** (2.15 Å), and a chloride in **3** (2.40 Å). Ru^{II}−Cl and Ru^{II}−N bond lengths are in agreement with values reported previously for arene complexes.[45,46]

All three complexes crystallized with four molecules in the unit cell. The biphenyl unit is twisted by 54° and 52° in **1·HCl** and **3**, respectively, and 85° in **2**. Adjacent molecules crystallized with their bound arenes parallel to each other. The extended crystal structure of **1·HCl** showed intermolecular $\pi-\pi$ stacking of the unbound arenes with a distance between arene centroids of 3.65 Å, and

Table 1. Crystallographic Data for $[Ru^{II}(\eta^6\text{-}C_6H_5(C_6H_4)NH_3)Cl_3]$, **1·HCl**, $[Ru^{II}(\eta^6{:}\eta^1\text{-}C_6H_5(C_6H_4)NH_2)(en)]Cl_2$, **2**, and $[Ru^{II}(\eta^6\text{-}C_6H_5(C_6H_4)NH_2)Cl(en)]Cl$, **3**

	1·HCl	**2**	**3**
formula	$C_{12}H_{12}Cl_3NRu$	$C_{14}H_{19}Cl_2N_3Ru$	$C_{14}H_{19}Cl_2N_3Ru$
MW	377.66	401.30	401.29
crystal description	red block	yellow block	orange block
crystal size (mm)	0.61 × 0.49 × 0.24	0.48 × 0.23 × 0.20	0.24 × 0.23 × 0.23
λ (Å)	0.71073	0.71073	0.71073
T (K)	150	150	150
crystal system	monoclinic	orthorhombic	monoclinic
space group	$P2_1/n$	$P2_12_12_1$	$P2_1/c$
a (Å)	13.1377(4)	9.0448(2)	11.5327(9)
b (Å)	6.8928(2)	11.0210(3)	9.2986(7)
c (Å)	15.0526(5)	15.7360(4)	14.9108(11)
α (deg)	90	90	90
β (deg)	110.648(2)	90	108.770(5)
γ (deg)	90	90	90
vol (Å^3)	1275.54(7)	1568.61(7)	1514.0(2)
Z	4	4	4
$R\,[F > 4\sigma(F)]^a$	0.0235	0.0186	0.0401
$R_w{}^b$	0.0618	0.0485	0.1081
GOF^c	1.0634	0.7529	1.050
$\Delta\rho$ max and min (e Å^{-3})	0.61 and −0.65	0.39 and −0.30	1.286 and −1.335

$^a R = \sum||F_o| - |F_c||/\sum|F_o|$. $^b R_w = [\sum w(F_o^2 - F_c^2)^2/\sum wF_o^2]^{1/2}$. ^{c} GOF $= [\sum[w(F_o^2 - F_c^2)^2]/(n-p)]^{1/2}$, where n = number of reflections and p = number of parameters.

Table 2. Selected Bond Lengths (Å) and Angles (deg) for Complexes **1·HCl**, **2**, and **3**

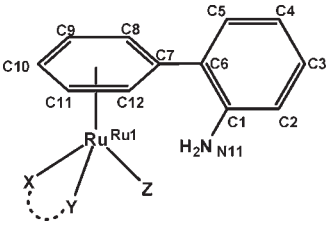

	1·HCl	**2**	**3**
X	Cl3	N12	N12
Y	Cl2	N42	N42
Z	Cl1	N11	Cl1

bond length (Å)/ angle (deg)^a	**1·HCl**	**2**	**3**
Ru1−X	2.4053(5)	2.1368(17)	2.120(4)
Ru1−Y	2.4367(4)	2.1196(17)	2.141(4)
Ru1−Z	2.4175(5)	2.1481(17)	2.4006(12)
Ru1−C7	2.1970(18)	2.113(2)	2.238(5)
Ru1−C8	2.1798(18)	2.188(2)	2.200(5)
Ru1−C9	2.1799(18)	2.197(2)	2.182(5)
Ru1−C10	2.1591(18)	2.206(2)	2.166(5)
Ru1−C11	2.1707(18)	2.195(2)	2.162(5)
Ru1−C12	2.1721(19)	2.185(2)	2.173(5)
C1−N11	1.466(2)	1.464(2)	1.406(6)
C6−C7	1.489(2)	1.501(3)	1.483(7)
X−Ru1−Y	87.049(16)	79.85(7)	79.36(15)
X−Ru1−Z	87.532(17)	89.87(6)	85.95(11)
Y−Ru1−Z	86.288(17)	86.63(7)	85.77(11)
dihedral angle	54.48	85.15	51.83
Ru1-centroid^b	1.647	1.654	1.666
offset C6^c	<0.02 (+)	0.488 (-)	0.055 (+)

^{a} Atom labeling scheme used for purposes of comparison only. The crystallographic atom labeling schemes for individual complexes are different and specified in Figure 1. ^{b} Measured using Mercury 1.4.1. ^{c} Offset of C6 with respect to the plane formed by bound arene (carbons C7−C12). (+) away from ruthenium; (-) toward ruthenium.

(45) Morris, R. E.; Aird, R. E.; Murdoch, P. d. S.; Chen, H.; Cummings, J.; Hughes, N. D.; Parsons, S.; Parkin, A.; Boyd, G.; Jodrell, D. I.; Sadler, P. J. *J. Med. Chem.* **2001**, *44*, 3616–3621.

(46) Chen, H.; Parkinson, J. A.; Parsons, S.; Coxall, R. A.; Gould, R. O.; Sadler, P. J. *J. Am. Chem. Soc.* **2002**, *124*, 3064–3082.

between parallel planes of 3.35 Å (Supporting Information, Figure S3). The two rings are offset such that the ring normal and the vector between the arene centroids form an angle of 22°. The crystal structure of complex **3** did not show $\pi-\pi$ stacking, despite the fact that the unbound phenyl rings are parallel. The dihedral angle between the two quasi-parallel rings is 3.5°. The chloride ligands in **1·HCl** are extensively involved in H-bonding with the NH_3(tether) hydrogens (N−H···Cl distance 2.25−2.53 Å). In complex **3**, the chlorides (both counterion and ligand) are involved in H-bonding to the NH_2(tether) hydrogen atoms (N−H···Cl distances of 2.55 and 2.61 Å) and to the hydrogen atoms on the NH_2(ethylenediamine) ligand (N···Cl distances in the range 3.10−3.47 Å). In complex **2**, the chloride counterions also appear to be involved in H-bonding to the ethylendiamine ligand (N···Cl distances 3.17 and 3.26 Å) or the NH_2(tether) (N···Cl distances 3.24 and 3.25 Å).

The DFT optimized structures of **2** and **3** are in agreement with the X-ray data, although both the functionals employed tend to overestimate bond distances (B3LYP in particular). When a Cl^- counterion is included in the geometry optimization of **2**, [**2**+**Cl**], the computed bond distances have a better agreement with the experimental ones (Supporting Information, Table S1). Interestingly, energy comparison between the structure of closed-tether [**2**+**Cl**] and open-tether **3** in the gas phase shows that the latter is about 17 kcal/mol more stable (Supporting Information, Figure S4). Furthermore, DFT calculations show that the closed-tether **2** (calculated as [**2**+$\mathbf{H_2O}$]) is 5.8 kcal/mol more stable than its open form coordinating a H_2O molecule, [**5**+**H**] (Supporting Information, Table S1).

Solution Studies of the Tethered-Arene Chelate. The dynamics of the tethered-arene chelate in different solvents were investigated by NMR spectroscopy.

In $(CD_3)_2SO$, complex **2** formed the open-tethered DMSO adduct complex **4**, $[Ru(\eta^6\text{-}C_6H_5(C_6H_4)NH_2)(DMSO\text{-}d_6)(en)]^{2+}$, over 18 h. The NH_2 on the pendant arm of the arene ligand dissociated from the ruthenium and was substituted by a molecule of DMSO. The ESI-MS fragment observed at 449.33 m/z is assignable to the species $\{C_{16}H_{18}D_6ClN_3ORuS\}^+$, confirming formation of cation **4** (Supporting Information, Figure S5). The conversion of complex **2** into complex **4** in DMSO-d_6 was followed by NMR spectroscopy. The data were obtained by integration of ^{1}H NMR peaks in spectra recorded at various time intervals at 298 K and were fitted to pseudo-first order reaction kinetics (Figure 2). At 298 K, the rate constant for this reaction is $4.81 \pm 0.23 \times 10^{-5}$ s^{-1}, and the half-life is about 4 h (237 min). The spectrum showed little change when the sample was kept at ambient temperature for a period of 10 days.

In methanol, complex **2** formed the open-tethered monocation complex **3** within 12 h. The Ru−N bond involving the pendant arm NH_2 is dissociated, and the amine is substituted by a chloride ligand (two equivalents present in solution, as counterions of the ruthenium-arene dication complex **2**). The time-course reaction was followed by ^{1}H NMR spectroscopy, and the data for the conversion of **2** into **3** in methanol were fitted to a single-exponential function (Figure 3). At 298 K, the half-life is about 5 h. Complexes **3** and **2** exist in equilibrium in a ratio 70% to 30%, respectively. The recorded ^{1}H NMR spectra showed little change even when the sample was kept at room temperature for 50 days.

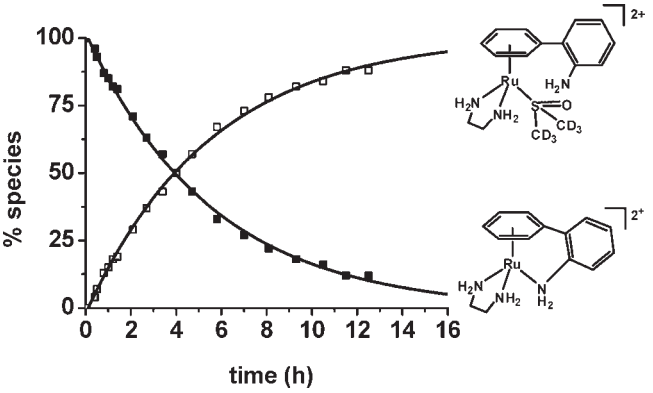

Figure 2. Conversion over time of $[Ru^{II}(\eta^6{:}\eta^1\text{-}C_6H_5(C_6H_4)NH_2)(en)]^{2+}$, **2** (2.9 mM; black squares) into $[Ru^{II}(\eta^6\text{-}C_6H_5(C_6H_4)NH_2)(DMSO\text{-}d_6)(en)]^{2+}$, **4** (white squares), over time at 298 K by displacement of the NH_2 group in the tether arm of **2** by a molecule of solvent in DMSO-d_6. The solid lines represent computer best fits of a pseudo-first order reaction giving a rate constant of $4.81 \pm 0.23 \times 10^{-5}$ s^{-1}.

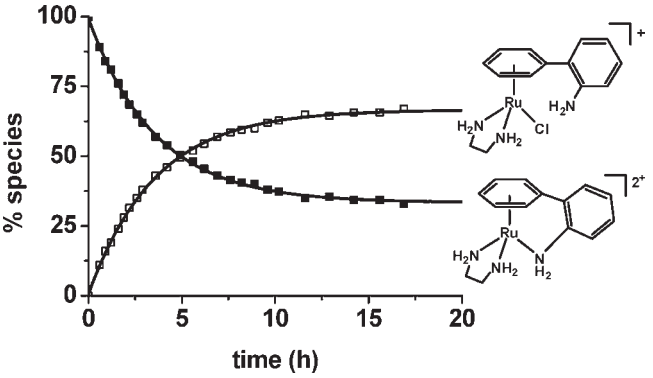

Figure 3. Relative populations in methanol solution of $[Ru^{II}(\eta^6{:}\eta^1\text{-}C_6H_5(C_6H_4)NH_2)(en)]^{2+}$, **2** (2.9 mM; black squares), and $[Ru^{II}(\eta^6\text{-}C_6H_5(C_6H_4)NH_2)Cl(en)]^{+}$, **3** (white squares), over time at 298 K by displacement of the NH_2 group in the tether arm of **2** by a chloride ion. The plots show fits to single-exponential functions giving a half-life of about 5 h.

When complex **2** was dissolved in water no change was observed in the ^{1}H NMR spectrum up to a period of 3 days at pH about 7. When complex **3** was dissolved in water, however, it was fully converted to complex **2** within 2 h (Figure 4). The conversion of the open-tether complex **3** into closed-tether complex **2** in water was followed by ^{1}H NMR spectroscopy. The time-course data were fitted to first-order kinetics. At 298 K, the rate constant of this reaction is $4.71 \pm 0.11 \times 10^{-4}$ s^{-1} with a half-life of 24 min.

An aliquot of an aged DMSO solution containing the open-cation $[Ru(\eta^6\text{-}C_6H_5(C_6H_4)NH_2)(DMSO)(en)]^{2+}$ (**4**) was diluted with D_2O to a final concentration of 10% DMSO. Within 2 h complex **4** was totally converted to the closed form **2** (Supporting Information, Figure S6). At 298 K, the rate constant for this first order reaction is $5.59 \pm 0.10 \times 10^{-4}$ s^{-1} with a half-life of 20 min. When an aliquot of the aged DMSO solution was diluted into brine (prepared in D_2O) to a final concentration of 10% DMSO, complex **2** formed over time and equilibrium was reached after about 4 h (see Supporting Information,

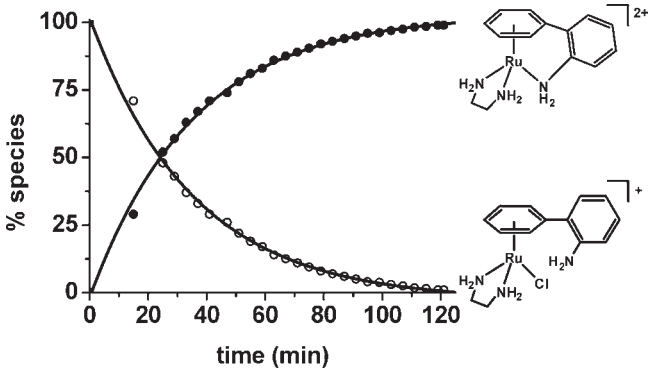

Figure 4. Conversion of $[Ru^{II}(\eta^6\text{-}C_6H_5(C_6H_4)NH_2)Cl(en)]^+$, **3** (2.9 mM; white circles) into $[Ru^{II}(\eta^6{:}\eta^1\text{-}C_6H_5(C_6H_4)NH_2)(en)]^{2+}$, **2** (black circles), over time at 298 K by displacement of the chloride ligand in **3** by the NH_2 group in the tether arm to form **2** in water. The plots represent computer best fits of a first order reaction giving a rate constant of $4.71 \pm 0.11 \times 10^{-4}$ s^{-1}.

Figure S7). At equilibrium, the ratio of the two complexes **2**:**4** was 87%:13%. The equilibrium constant was 6.7 at 298 K.

Effect of pH. Acid Titration. Complex **2** was dissolved in H_2O/D_2O (9:1) (ca. 2.9 mM). ^1H NMR peaks of complex **2** did not shift or vary in intensity throughout the pH range 7−2, nor over 24 h at pH 2. The tether chelate opened when complex **2** was reacted in 12 M HCl for 18 h. The NH_2 group of the pendant arm dissociated from ruthenium and was protonated to give $[Ru(\eta^6\text{-}C_6H_5(C_6H_4)NH_3)Cl(en)]^{2+}$. This assignment was based on analysis of the ^1H NMR signals of an aliquot of the acidic solution diluted with DMSO-d_6 (Supporting Information, Figure S8), and comparison with those of complex **4** in DMSO-d_6.

Base Titration. A new set of ^1H NMR peaks appeared during the titration of **2** with NaOH, over the pH range 6−12 (Figure 5). At pH 9, a complete set of new signals was observed, and their intensity increased as the solution approached pH 12. The new signals were attributed to the formation of an open-tether complex on the basis of the chemical shift pattern. The species was assigned as complex **5**, $[Ru(\eta^6\text{-}C_6H_5(C_6H_4)NH_2)(en)(OH)]^+$.

The increase in intensity of the resonance peaks of complex **5** was accompanied by a concurrent decrease in the intensity of peaks for complex **2**, which disappeared altogether at about pH 12. Incidentally, the diminishing peaks of **2** also shifted toward higher field as pH 12 was approached.

The conversion of **2** into **5** was fully reversible, as shown by NMR spectroscopy. On neutralization of the basic solution with dilute HNO_3, the ^1H NMR signals corresponding to complex **2** reappeared, while those signals attributed to complex **5** disappeared.

The pH-effect on complex **2** was also followed by UV−vis spectroscopy (Figure 6). Assignment of the UV−vis spectrum of **2** was obtained through calculating 32 singlet transitions with the TD-DFT method (Supporting Information, Figures S9−S11). The low-energy band at 340 nm is metal-centered in character, as well as the more intense band at about 300 nm. The highest energy band is mainly composed of transitions with a metal-to-ligand charge-transfer character, where electron density migrates from the metal center to the 2-aminophenyl ligand.

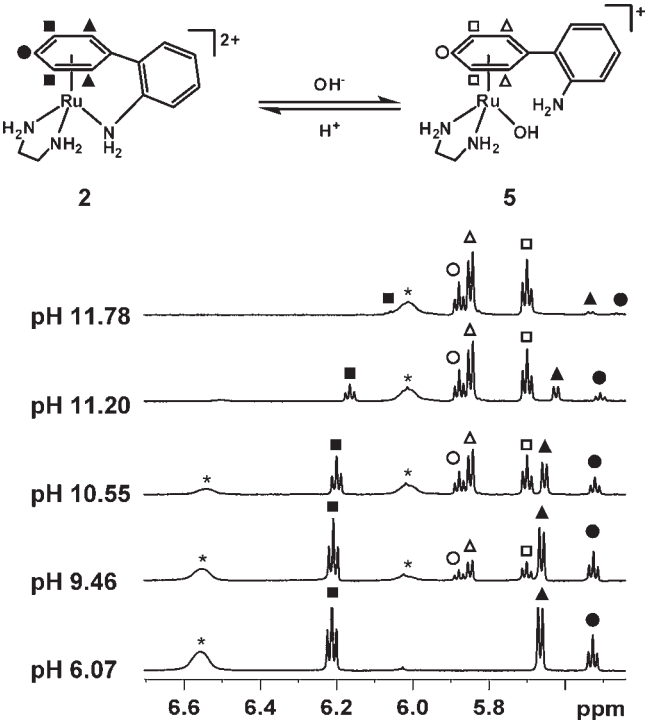

Figure 5. pH dependence of the signals corresponding to the η^6-bound arene region of ^1H NMR spectra of $[Ru^{II}(\eta^6{:}\eta^1\text{-}C_6H_5(C_6H_4)NH_2)(en)]Cl_2$, **2**, in H_2O/D_2O (9:1). Refer to the structure for assignment of the arene signals. *The broad NMR peaks at 6.6 ppm and 6.0 ppm correspond to the ethylenediamine NH_u protons (protons pointing up toward the η^6-arene) of **2** and **5**, respectively.

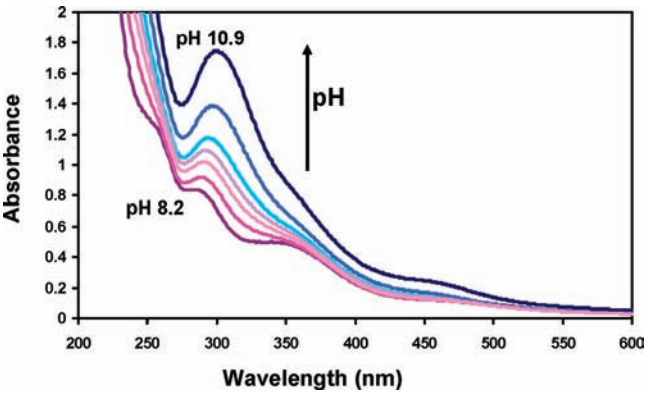

Figure 6. Changes in absorbance in the range 200−600 nm upon increasing pH in an aqueous solution of complex **2** (0.8 mM) at 298 K. The band at about 300 nm is assignable to complex **5**.

The basic titration (pH range 6−12) of the aqueous solution of **2** showed an increase in the absorbance band at about 300 nm as the pH was increased. Such behavior is consistent with the opening of the tethered complex **2** and the formation of **5**. The TD-DFT predicted UV−vis spectrum of **5** showed, in fact, an intense ligand-centered (2-aminophenyl) transition at 309 nm (Supporting Information, Figures S12 and S13). Similarly, the calculated UV−vis spectrum of the open-tether complex **3** had an intense ligand-centered band in the same region (Supporting Information, Figures S14 and S15). When the pH was decreased to pH 8, the bands in the experimental spectrum decreased in intensity to those of the initial UV−vis trace, showing complete reversibility, in agreement with

the results obtained by NMR. Further acidification of the solution to pH 3 did not result in any further change to the UV−vis spectrum.

Discussion

As a potential strategy for the controlled activation of Ru^{II} arene anticancer complexes, we have synthesized tethered complexes which, upon dissociation of a $Ru^{II}-N_{tether}$ bond, offer a vacant site for biomolecule interaction. Dissociation is promoted by the strain generated by the 5-membered chelate ring and is aided by solvent coordination. Tether ring-opening is a potentially useful concept in anticancer drug design.

Synthesis, Stability, and Characterization. The arene exchange reaction used to obtain complex **1** from the dimer $[Ru(\eta^6\text{-etb})Cl_2]_2$ appears to be favored in 1,2-dichloroethane at high temperatures in a pressure vessel.[10] Almost quantitative yields were achieved under the above conditions. The mechanism by which pressure influences the yield is not clear. However, it could assist in overcoming activation barriers between the tether arene and the ruthenium center.

The neutral dichlorido complex **1**, $[Ru^{II}(\eta^6{:}\eta^1\text{-}C_6H_5(C_6H_4)NH_2)Cl_2]$, appeared to be insoluble in most common solvents, whereas related complexes, such as $[Ru^{II}(\eta^6\text{-}p\text{-cymene})Cl_2(p\text{-methylaniline})]$, and $[Ru^{II}(\eta^6\text{-benzene})Cl_2(p\text{-methylaniline})]$ are reported to be soluble in dichloromethane and/or in chloroform.[47,48] After prolonged sonication, complex **1** appeared to dissolve in DMSO-d_6 but detailed examination of the ^1H NMR spectrum showed a chemical shift pattern consistent with the open tether $[Ru^{II}(\eta^6\text{-}C_6H_5(C_6H_4)NH_2)Cl_2(DMSO)]$, where the NH_2(tether) in **1** was displaced by a DMSO molecule.

Detailed analysis of NMR signals of the Ru^{II} complexes showed similar chemical shift patterns for the ^1H NMR signals of the open- (**1·HCl**, **3**, **4**, and **5**) and closed- (**2**) tethers in different solvents. The chemical shifts of the proton resonances of the η^6-arene and phenyl ring protons in the pendant arm turned out to be useful markers to follow the dynamics of tether ring-opening and closing in solution.

Strongly coordinating solvents such as acetonitrile or DMSO are known to be capable of displacing arenes from Ru^{II} complexes such as $[Ru(\eta^6\text{-arene})Cl_2(L)]$. These complexes are often not stable in such solvents and can convert totally to species such as $[RuCl_2(solvent)_4]$,[49] or lose the arene upon oligonucleotide coordination as shown for complexes where the arene is benzene, *p*-cymene, phenylethyl alcohol, or *N*,*N*-dimethylbenzylamine and L is a phosphine derivative, such as PTA.[7] Arene-loss-related decomposition has also been documented for tethered Ru^{II}-arene complexes with 5-membered tethered rings, such as $[Ru^{II}(\eta^6{:}\eta^1\text{-}C_6H_5(CH_2)_2NH_2)Cl(phosphine)]^+$,[7] and $[Ru^{II}(\eta^6{:}\eta^1\text{-}C_6H_5(CH_2)_2NH_2)Cl_2]$.[9] The phosphine-containing tethered complex undergoes more arene-loss than open-tether analogues. DFT calculations have not been able to correlate this reactivity with the strength of the Ru-arene bond.[7] It has been suggested that a more rigid tether backbone would decrease the stability of the Ru-coordinated arene and lead to arene loss by weakening of the Ru^{II}-η^6-arene bond.[10] Melchart et al. observed an improvement in the stability of the coordinated arene in the complex $[Ru^{II}(\eta^6{:}\eta^1\text{-}C_6H_5(CH_2)_2NH_2)(oxalate)]$ (only ca. 16% decomposed in 24 h) in comparison to its dichlorido analogue $[Ru^{II}(\eta^6{:}\eta^1\text{-}C_6H_5(CH_2)_2NH_2)Cl_2]$ (fully decomposed within 8 h).[10] The improvement was attributed to the stabilizing effect of the bidentate oxalate ligand. In the present work arene-loss related decomposition was not observed for **2** in any of the solvents used. The stabilization gained by the presence of the chelating ethylenediamine leads to a ruthenium center fixed in a rigid and stable bicyclical framework and may account for the strong binding between ruthenium and the arene in **2**.

X-ray Crystal Structures. The structural constraints within the closed-tether complex **2** are apparent from the orientation of the two phenyl rings which are almost perpendicular to each other with a dihedral or torsion angle of 85°, in comparison with the smaller biphenyl twists of 54° and 52° in **1·HCl** and **3**, respectively. The replacement of the NH_2 group of the pendant arm by a phosphino group does not appear to show structural differences with regard to the biphenyl twists (69−88°).[50−56] However, the distances between the centroids of the bound arenes and the ruthenium centers appear to be longer (ranging from 1.684 to 1.791 Å) than in **2** (1.654 Å). Further evidence for the strain within the structure of **2** is the observation that the distance between the central ruthenium atom and the NH_2 group of the pendant arm (2.148 Å) is significantly longer than those of the Ru−N bonds of ethylenediamine in the same complex (2.120 and 2.137 Å). In addition, the differences in the distances between $Ru-C_{ipso}$ and $Ru-C_{para}$ for the η^6-bound arene (Ru1−C7 and Ru1−C10 in Table 2) are 0.04, 0.09, and 0.07 Å for **1·HCl**, **2**, and **3**, respectively, suggesting that the tilt in the η^6-bound arene is more pronounced for **2** than for the other open-tethered complexes **1·HCl** and **3**. The tilt is toward the *ipso* carbon only for **2** in this work and not for complexes **1·HCl** and **3**. This is again attributable to the constraints imposed by the closure of the tethered arm. A similar tilt has been reported for the crystal structure of a related analogue $[Ru^{II}(\eta^6{:}\eta^1\text{-}C_6H_5(C_6H_4)NH_2)(oxalate)]$.[10] Conformational constraints have been reported in aliphatic two-carbon tethers compared with less strained three- and four-carbon tethers, which has been related to the difference in catalytic activity in asymmetric hydrogenation of aromatic ketones.[57]

The relatively short distance observed for C1−N11 in **3** (1.407 Å) compared to **1·HCl** (1.466 Å) and **2** (1.464 Å) is

(47) Bates, R. S.; Begley, M. J.; Wright, A. H. *Polyhedron* **1990**, *9*, 1113–1118.
(48) Begley, M. J.; Harrison, S.; Wright, A. H. *Acta Crystallogr., Sect. C: Cryst. Struct. Commun.* **1991**, *C47*, 318–320.
(49) Valerga, P.; Puerta, M. C.; Pandey, D. S. *J. Organomet. Chem.* **2002**, *648*, 27–32.
(50) den Reijer, C. J.; Woerle, M.; Pregosin, P. S. *Organometallics* **2000**, *19*, 309–316.
(51) Faller, J. W.; D'Alliessi, D. G. *Organometallics* **2003**, *22*, 2749–2757.
(52) Faller, J. W.; Fontaine, P. P. *Organometallics* **2005**, *24*, 4132–4138.
(53) Faller, J. W.; Fontaine, P. P. *Organometallics* **2007**, *26*, 1738–1743.
(54) Faller, J. W.; Fontaine, P. P. *J. Organomet. Chem.* **2007**, *692*, 976–982.
(55) Faller, J. W.; Fontaine, P. P. *J. Organomet. Chem.* **2007**, *692*, 1110–1117.
(56) Aikawa, K.; Kaito, I.; Mikami, K. *Chem. Lett.* **2007**, *36*, 1482–1483.
(57) Ito, M.; Komatsu, H.; Endo, Y.; Ikariya, T. *Chem. Lett.* **2009**, *38*, 98–99.

consistent with the absence of coordination/protonation of the NH_2(tether), since C−NH_2 distances appear to be shorter when the lone pair of electrons on the nitrogen is not involved in coordinative or covalent binding.[58−60] The presence of an NH_2-ended tether in a metal complex, which is neither coordinated to the metal center nor protonated is unprecedented, all other examples in the literature appear to show the metal-free amino-tether protonated.[7,8,61]

Solution Chemistry. The driving force for tether-opening is thought to be the relaxation of strain imposed by the rigid five-membered ring containing an aromatic backbone, together with the coordination of a monodentate ligand. The higher extent of formation of the ring-opened complex **3** in methanol is consistent with the results obtained by DFT calculations in the gas phase, which showed a higher stability for **3** compared to [**2**+**Cl**] (ca. 17 kcal/mol) (Supporting Information, Figure S4). Mijaki et al. have reported that complexes of general formula [Ru(η^6:η^1-$C_6H_5(CH_2)_3OH$)Cl(PR_3)]BF_4 (R = Ph or Et) and [Ru(η^6:η^1-$C_6H_5(CH_2)_3OH$)(N,N')]$(BF_4)_2$ ring-open in the presence of Cl^- to give the open-tether chlorido complexes in almost quantitative yields. The reason for this facile ring-opening is the weakness of the metal−oxygen bond. Amino chelate complexes such as [Ru(η^6:η^1-$C_6H_5(CH_2)_n$-NH_2)Cl(PPh_3)]BF_4 (n = 2, 3), however, remained in their closed state in the presence of chloride ions.[8] Melchart et al. observed the same stability vis-à-vis tether-opening for the two- and three-carbon tethered complexes of formula [Ru(η^6:η^1-$C_6H_5(CH_2)_nNH_2$)Cl_2] (n = 2, 3), where the release of the ring strain in DMSO came about through dissociation of the η^6-arene (more extensive and faster for the more strained two-carbon tether), but not through dissociation of the Ru−N_{tether} bond. Mijaki et al. also reported the open-tether complex [Ru(η^6-C_6H_5-$(CH_2)_2N(CH_3)_2$)Cl_2(PPh_3)], where closure of the chelating tether was not favorable because of the steric hindrance imposed by a tertiary amine.[8,62] Scolaro et al. showed that the complex [Ru(η^6-$C_6H_5(CH_2)_2NH_3$)Cl_2-(phosphine)]Cl can only be maintained in a tether-open state by protonation.[7] In the case of **2**, acid titration (down to pH 2) and keeping the solution at that pH for 24 h did not result in ring-opening. This could only be achieved by the use of a large excess of hydrochloric acid (12 M) over 18 h, resulting in the formation of [Ru(η^6-$C_6H_5(C_6H_4)NH_3$)Cl(en)]$^{2+}$. These results suggest that the opening of the tether under acidic conditions is thermodynamically favorable but kinetically slow. Habtemariam et al. reported the chelate ring-opening dynamics of aminophosphine complexes of general formula [M($R^1R^2N(CH_2)_nPPh_2$)$_2$]$^{2+}$, (M = Pt^{II} or Pd^{II}) in water,[11] and were able to control ring-opening and -closure by factors such as ring size (n = 2 or 3) and substituents on the coordinating nitrogen atom (R^1 and R^2 = H, Me, benzyl, cyclohexyl). The *trans* effect of the phosphino group contributed to opening the ring by weakening of the Pt−N bond. In the case of the chelating rings containing primary amines, ring-opening was induced by protonation of the amine group.[11]

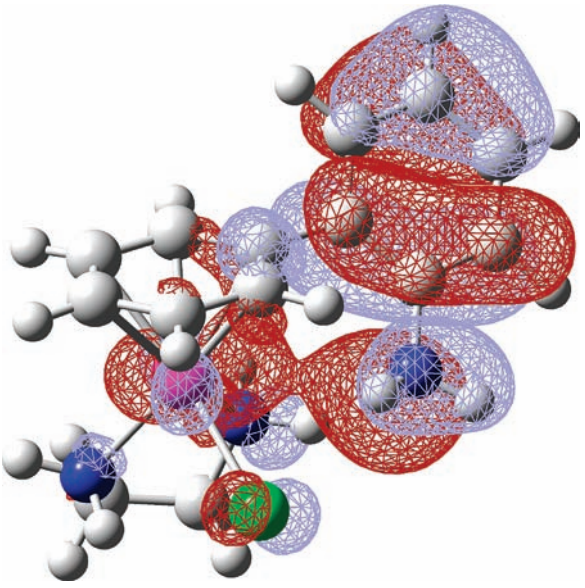

Figure 7. HOMO orbital of complex **3** (PBE1PBE/LanL2DZ/6-31G**, isovalue 0.02).

Ring-closure of the tether appears to be highly favored in aqueous solution (neutral pH) as shown by the short half-life (24 min) for the conversion of chlorido complex **3** to tethered complex **2** in water and DMSO complex **4** to **2** in DMSO/water (1:9) (20 min, 298 K), which involve displacement of chloride and DMSO (Figure 4 and Supporting Information, Figure S5), respectively, by the tether arm amino group. In the presence of a large excess of chloride ions, the chelation of the tether was inhibited by up to 13% (Supporting Information, Figure S6), which highlights the competition of the Cl^- ions with the NH_2(tether) for the vacant site on the ruthenium center. The DFT calculations showed that the highest occupied molecular orbital (HOMO) orbital of complex **3** has an overlap between a p orbital of the NH_2 group and a d orbital of the metal center (Figure 7). This interaction may readily promote the closing of the tether under aqueous conditions, where Cl^- release is facilitated.

At basic pH (9−12) formation of the hydroxido complex **5** was observed as a result of nucleophilic attack by hydroxide on the ruthenium center in a concerted event likely assisted by H-bonding. Complete tether-ring-opening interconversion of **2** into **5** occurs at pH 12 (Figure 5). Such behavior was unexpected as protonation of the NH_2 group was believed to be crucial for the Ru−N bond dissociation (vide supra).

In addition, there is NMR evidence of a deprotonation process occurring for **2** at pH values approaching 12. However, the pK_a could not be determined by ^{1}H NMR spectroscopy on account of the decrease in intensity and complete disappearance of the ^{1}H NMR signals during the titration under these basic conditions.

Decreasing the pH from basic to neutral values is likely to trigger in the first instance protonation of the hydroxido ligand in **5.** Aqua adducts of ethylenediamine Ru^{II}

(58) Smith, G.; Wermuth, U. D.; White, J. M. *Acta Crystallogr., Sect. C: Cryst. Struct. Commun.* **2006**, *C62*, o402–o404.
(59) Zhang, S. F.; Sun, Y. Q.; Yang, G. Y. *Acta Crystallogr., Sect. C: Cryst. Struct. Commun.* **2004**, *C60*, m299–m301.
(60) Upreti, S.; Ramanan, A. *Inorg. Chim. Acta* **2005**, *358*, 1241–1246.
(61) Habtemariam, A.; Parkinson, J. A.; Margiotta, N.; Hambley, T. W.; Parsons, S.; Sadler, P. J. *J. Chem. Soc., Dalton Trans.* **2001**, 362–372.
(62) Meyerstein, D. *Coord. Chem. Rev.* **1999**, *185−186*, 141–147.

arene complexes in general have high pK_a values (ca. 8).[63] Protonation of the hydroxido ligand in **5** could then lead to tether-closure since Ru−OH_2 bonds are normally reactive,[6] whereas Ru−OH bonds are relatively inert. Consistently, DFT calculations suggest that the energetic balance between [**2**+$\mathbf{H_2O}$] and [**5**+**H**] favors ring closure (5.8 kcal/mol). The reversibility of the process was fully confirmed by the UV−vis titration (Figure 6), indicating high stability of the system making the behavior of the arene-tether ligand comparable with that of previously described hemilabile ligands.[12]

Conclusions

The versatile coordination properties of an amino-derivatized arene have been investigated in different solvents. We have shown that constraints of a five-membered ruthenium(II) tether ring (enhanced by a rigid aromatic backbone), formed by an η^6-arene ligand and pendant η^1-donor atom, can be tailored to weaken the otherwise strong (nonlabile) Ru^{II}−NH_2(tether) bond in [$Ru^{II}(\eta^6{:}\eta^1$-$C_6H_5(C_6H_4)NH_2)$-(en)]Cl_2 (**2**). This complex is stable as no arene-loss was observed under highly acidic or basic conditions or in different solvent systems. In methanol, complex **2** can exist as an equilibrium between open- (activated) (**3**) and closed- (inactivated) (**2**) tether forms. In DMSO, **2** can open to form **4**. In addition, **2** opens both in concentrated hydrochloric acid, and in water at pH 12.

Conveniently, **2** opens to form **3**, **4**, or **5** without requiring protonation of the primary amine, $-NH_2$, which remains available for further interactions, for example C-terminal labeling of amino acids and peptides,[64] or other biological substrates, and organic polymers.

The solution behavior of the closed-tether complex **2** supports the concept that it is possible to synthesize ruthenium arene prodrugs which will allow activation upon tether-opening only under specific conditions. Most importantly, the activation/deactivation process is fully reversible and complex **2** does not undergo arene-loss decomposition in the solvents used in this work.

Further work will be directed toward the development of new $\eta^6{:}\eta^1$-arene:N hemilabile ligands with finely tuned electronic and steric properties so that activation of tethered ruthenium organometallic arene complexes can be controlled under biologically relevant conditions. Control over the opening and closure of the tether ring as a function of pH might provide a Ru-arene complex which is specifically activated in cancer cells.[14]

The possible contributions of these systems as catalysts, or their exploitation in other applications where complexes containing other metal-hemilabile ligands are being successfully developed, for example, as small molecule sensors,[65] or as a tool in supramolecular chemistry,[66] have yet to be explored.

Acknowledgment. This research was supported by the EC (Marie Curie Intra European Fellowships for A.M.P. (515560 METCOMDPLINK) and L.S. (220281 PHOTORUACD) within the 6th and 7th European Community Framework Programmes, respectively), and by Science City (AWM and ERDF). We thank the EPSRC and The University of Edinburgh for a studentship for M.M., and members of EC COST Action D39 for stimulating discussions.

Supporting Information Available: Computational details (tables of selected bond lengths and angles, molecular orbitals and absorption spectra), kinetic, MS and NMR data. This material is available free of charge via the Internet at http://pubs.acs.org.

(63) Wang, F.; Chen, H.; Parsons, S.; Oswald, I. D. H.; Davidson, J. E.; Sadler, P. J. *Chem.—Eur. J.* **2003**, *9*, 5810–5820.
(64) Stodt, R.; Gencaslan; Müller, I. M.; Sheldrick, W. S. *Eur. J. Inorg. Chem.* **2003**, 1873–1882.
(65) Angell, S. E.; Zhang, Y.; Rogers, C. W.; Wolf, M. O.; Jones, W. E., Jr. *Inorg. Chem.* **2005**, *44*, 7377–7384.
(66) Khoshbin, M. S.; Ovchinnikov, M. V.; Mirkin, C. A.; Zakharov, L. N.; Rheingold, A. L. *Inorg. Chem.* **2005**, *44*, 496–501.